Eur Biophys J (1997) 26: 209–214

ARTICLE

Mattia Filiaci · G. Ulrich Nienhaus

The role of entropy in the discrimination between CO and O_2 in myoglobin

Received: 13 January 1997 / Accepted: 24 April 1997

Abstract Using stopped-flow rapid mixing and flash photolysis techniques, the dissociation rate coefficients of horse carbonmonoxy myoglobin (hMbCO) and oxygenated myoglobin ($hMbO_2$) in aqueous solution have been determined as a function of temperature between 274 and 342 K. From the Arrhenius plot, an activation enthalpy for dissociation of 74 kJ/mol was obtained for both ligands. The pronounced kinetic differences arise from markedly different pre-exponentials. We compare the Arrhenius parameters with those of the association reaction, as measured at cryogenic temperatures. In our analysis we conclude that the entropy loss upon binding of O_2 is twice as large as that for CO. Taking reasonable estimates for the frequency factor, the transition state entropy in $hMbO_2$ is located roughly half way in between the entropies of the bound and unbound states. By contrast, the entropy of the transition state in hMbCO appears to be identical to that of the bound state. Possible structural reasons for the different behavior are discussed.

Key words Ligand binding · Myoglobin · Reaction rates · Entropy

1 Introduction

All functional processes in living systems are based on chemical reactions that take place in the complex but highly organized environment provided by biological macromolecules. To understand biology at the molecular level, we need to know how the reaction rates are controlled and fine-tuned. Heme proteins offer unique advantages for these studies, and consequently, ligand binding to heme proteins is most likely the single best-studied chemical reaction in the condensed phase (Frauenfelder and Wolynes 1985). The small, monomeric myoglobin (Mb), is a particularly useful model system, and myoglobins of many different species and many mutants have been characterized structurally (Phillips 1980; Kuriyan et al. 1986; Schlichting et al. 1994; Yang and Phillips 1996). Functional aspects have been studied in great detail using steady-state and time-resolved spectroscopic methods, including visible (Austin et al. 1975; Steinbach et al. 1991; Ansari et al. 1994), near-infrared (Campbell et al. 1987; Steinbach et al. 1991; Nienhaus et al. 1992; Lim et al. 1993), mid-infrared (Alben et al. 1982; Shimada and Caughey 1982; Mourant et al. 1993; Braunstein et al. 1993; Li et al. 1994; Nienhaus et al. 1994) and resonance Raman (Rousseau and Argade 1986; Champion 1988; Ahmed et al. 1991; Gilch et al. 1993) spectroscopies.

Ligand binding is a complex process that does not only involve motions of the ligand and the heme iron, but also conformational rearrangement of the entire protein globule. The basic features of the reaction can be described with the following scheme (Nienhaus et al. 1994; Nienhaus et al. 1995),

$$A \rightleftharpoons B^0 \rightleftharpoons B^3 \rightleftharpoons S\,. \tag{1}$$

Here, A represents the ligand-bound state. Immediately after ligand dissociation, the system is in state B^0, where the protein globule is in an intermediate, metastable state similar to A, and the ligand is in the heme pocket. From B^0, it can relax to the equilibrium unligated structure, with the ligand still in the heme pocket (state B^3). Finally, the ligand can exit to the solvent, and the protein is in the deoxy state (state S).

In this contribution, we focus on the final binding step, $A \rightleftharpoons B^0$, in the association and dissociation of carbon monoxide (CO) and dioxygen (O_2). Below 160 K, protein motions are mostly arrested, and the molecule remains in state B^0 after photodissociation until it returns to A upon recombination. Cryo-crystallographic studies of B^0 of MbCO have recently been performed (Schlichting et al. 1994; Teng et al. 1994; Hartmann et al. 1996). The rebind-

M. Filiaci · G. U. Nienhaus
Department of Physics, University of Illinois at Urbana-Champaign, 1110 West Green Street, Urban, IL 61801-3080 USA

G. U. Nienhaus (✉)
Department of Biophysics, University of Ulm, D-89069 Ulm, Germany (Fax: +49-731-502-3059; email: uli@uiuc.edu)

ing ($B^0 \rightarrow A$) can be conveniently studied by flash photolysis at low temperatures (Austin et al. 1975). The reverse reaction ($A \rightarrow B^0$) can only be studied at higher temperatures where thermal energy is sufficient to yield a reasonable rate of dissociation events [1]. In either direction, the temperature dependence of the rate coefficients is given by the Arrhenius law,

$$k = A\,(T/T_0)\,\exp\,[-H/RT]\,, \qquad (2)$$

where A is a pre-exponential factor, T is the absolute temperature and T_0 is a reference temperature set to 100 K. The activation enthalpy is denoted by H and the universal gas constant by R.

The ligand binding process involves motions of the nuclei and also spin-tunneling processes in the electronic subsystem. In many reactions, the electronic configuration adapts adiabatically to the positions of the nuclei, and the reaction proceeds on a single, adiabatic reaction surface. In some cases, for instance in reactions involving spin changes or electron transfer over long distances, the electronic subsystem cannot keep up with the nuclear motion, and its dynamics has to be taken into account in a nonadiabatic theory. The oxygen binding reaction involves a net spin change of one which implies a first-order spin-orbit interaction. This process should be sufficiently fast that an adiabatic approach is warranted. For CO binding, however, a spin change of two has to take place via the slower second-order spin-orbit interaction, and nonadiabatic theories have been put forward by Hopfield and collaborators (Redi et al. 1981) and Jortner and collaborators (Jortner and Ulstrup 1979; Buhks and Jortner 1985).

Frauenfelder and Wolynes (1985) pointed out that the electronic differences in the binding of CO and O_2 to sperm whale myoglobin (swMb) and hemoglobin chains should be reflected in pronounced differences in the Arrhenius parameters of the recombination reaction. Surprisingly, however, geminate recombination ($B \rightarrow A$) after photodissociation between 60 and 160 K shows very similar kinetics for MbO_2 and MbCO [2]. The fraction of molecules that have not rebound a ligand at time t after photodissocation, $N(t)$, can be described with a single distribution, $g(H_{BA})$, of activation barriers, so that

$$N(t) = \int g(H_{BA})\,\exp\,[-k_{BA}t]\;dH\,, \qquad (3)$$

with k_{BA} given by Eq. (2). The enthalpy barrier distributions for both ligands peak at $\approx$10 kJ/mol, and the pre-exponentials $A_{BA} \approx 10^9\ s^{-1}$. It was suggested that the presence of friction and intermediate states along the reaction coordinate renders the normally nonadiabatic CO recombination reaction adiabatic (Frauenfelder and Wolynes 1985).

Additional information about the $A \rightleftharpoons B$ transition can be obtained from the dissociation reaction. Measurements of dissociation rates of heme proteins have a long history. Early work was summarized by Gibson (1959), and an extensive compilation was given by Antonini and Brunori (1971). While rate coefficients at room temperature are often measured and reported, measurements of the temperature dependencies are much less frequently found. They are, however, most interesting if one wants to elucidate the details of the reaction mechanism. Here we have measured the temperature dependence of the rate coefficients for dissociation of CO and O_2 from horse myoglobin over as wide a temperature range as possible to determine the pre-exponentials and activation enthalpies of dissociation. While the association parameters for CO and O_2 are similar, the pre-exponentials for dissociation are in fact very different. Based on the assumption that the reaction surface that governs the final binding step is weakly dependent on temperature, we will show that the entropy difference between the unbound and bound states leads to the faster dissociation of dioxygen from myoglobin and discuss possible structural reasons for the difference.

2 Experimental Procedures

Samples of hMbCO and $hMbO_2$ were prepared by dissolving freeze-dried myoglobin powder in phosphate buffer (0.1 M, pH 7) and reducing with a three-fold excess of sodium dithionite solution under anaerobic conditions. The ligated forms were obtained by equilibration with 1 atm of CO or O_2. The final protein concentrations of the samples was $\approx$15 μM. For the stopped-flow experiments, phosphate buffer (0.1 M, pH 7) was equilibrated with 1 atm of CO or NO. The NO gas was washed in carbonate buffer (pH 10) prior to use.

To determine the ligand dissociation rates in hMbCO and $hMbO_2$, the protein solutions were rapidly mixed with a solution of the replacing ligand in a stopped-flow spectrometer (Kinetic Instruments, Bethesda, MD) equipped with a thermostatted water circulator (Haake, Paramus, NJ). NO was used to replace CO, and CO was used to replace O_2. The progress of the replacement reaction was monitored at a wavelength of 420 nm. At each temperature, between 3 and 10 kinetics traces were taken. Data were collected with a digital storage oscilloscope (model 3091; Nicolet, Madison, WI) linked to a Gateway 2000 PC.

Ligand association was studied with a flash photolysis system that employs a 6 ns (FWHM) wide pulse from a frequency-doubled, Q-switched Nd-YAG laser (532 nm, 300 mJ) for the photolysis (model NY-61, Continuum, Santa Clara, CA). Rebinding was monitored with light from a tungsten lamp that passed through a monochromator set at 440 nm. The light intensity was measured with a photomultiplier tube (model R 928; Hamamatsu Corp., Middlesex, NJ) and digitized with a home-made logarithmic-time-base digitizer (Wondertoy II) (Berendzen et al. 1989) from 1 μs to 100 s and a 500 MHz digital

[1] In the following, we shall drop the superscript '0' for simplicity, since we are not concerned with the protein relaxation here

[2] A substantial fraction of MbO_2 is not observed to recombine geminately on the nanosecond time scale and probably rebinds very fast (Petrich et al. 1988; Chance et al. 1990). This subpopulation is characterized by small out-of-plane displacements of the heme iron (Ahmed et al. 1991). We will not consider this component in our discussion

storage oscilloscope from 2 ns to 100 μs (model TDS 520; Tektronix, Wilsonville, OR). The sample was kept in a storage cryostat (model 10-DT; Janis Research Co. Inc., Wilmington, MA) equipped with a digital temperature controller (model DRC82C; Lake Shore Cryotronics Inc., Westerville, OH).

The apparent rate coefficients were extracted from both stopped-flow and flash photolysis data by least-squares fits of exponentials.

3 Determination of k_{AB}

The replacement reaction can be written as

$$\mathrm{MbL} + \mathrm{R} \underset{\lambda_L}{\overset{\lambda_{-L}}{\rightleftharpoons}} \mathrm{Mb} + \mathrm{L} + \mathrm{R} \underset{\lambda_{-R}}{\overset{\lambda_R}{\rightleftharpoons}} \mathrm{MbR} + \mathrm{L}\,, \qquad (4)$$

where L is the ligand that is initially bound, R is the replacing ligand, λ_{-L} and λ_{-R} are the overall dissociation rate coefficients, and λ_L and λ_R are the overall association rate coefficients. We use here pseudo-first-order rate coefficients because in our experiments the ligand concentration (≈1 mM) is much larger than the protein concentration (≈15 μM). For this scheme, the apparent rate coefficient, λ_{app}, in a stopped-flow experiment is given by (Olson, 1981)

$$\lambda_{app} = \frac{\lambda_{-L}\,\lambda_R + \lambda_{-R}\,\lambda_L + \lambda_{-L}\,\lambda_{-R}}{\lambda_L + \lambda_R + \lambda_{-R}}\,. \qquad (5)$$

In the replacement of CO by NO, NO binds about 70 times faster and dissociates about 200 times slower than CO. Thus, $\lambda_R \gg \lambda_L$, $\lambda_{-R} \ll \lambda_{-L}$, and Eq. (5) simplifies to

$$\lambda_{app} \approx \lambda_{-L}\,. \qquad (6)$$

Therefore, the apparent rate coefficient obtained from the CO/NO replacement reaction is in a very good approximation the overall CO dissociation rate coefficient.

In contrast, upon replacement of O_2 by CO, the replacing CO ligand has the smaller association rate, and simplifications cannot be applied to Eq. (5). Therefore, we measured the association rate coefficients λ_R and λ_L of the CO and O_2 ligands using flash photolysis. Taking the dissociation rate coefficient λ_{-R} of CO from the CO/NO replacement and the measured λ_{app} of the O_2/CO replacement, we calculated the overall dissociation rate coefficient λ_{-R} of O_2 with Eq. (5).

The overall dissociation rate coefficient represents those events where, after thermal cleavage of the iron-ligand bond, the ligand escapes into the solvent, where it subsequently competes with the replacing ligand for the vacant binding site. However, a certain fraction of ligands rebinds geminately, without leaving the protein. To obtain the microscopic dissociation rate coefficient, k_{AB}, which represents *all* bond-breaking events, we divide the overall dissociation rate coefficient by N_S, the fraction that escapes to the solvent after dissociation,

$$k_{AB} \approx \lambda_{-L}\,/N_S\,. \qquad (7)$$

The fraction N_S, extracted from the flash photolysis data on hMbCO and $hMbO_2$, is shown in Fig. 1. These data are in good agreement with earlier measurements by Chatfield et al. (1990). For hMbCO, nearly all ligands escape into the solvent after dissociation. Therefore, in the CO/NO replacement reaction, the CO dissociation rate coefficient k_{AB} is almost identical to λ_{-L} (and also λ_{app}). Figure 2 shows k_{AB} of hMbCO, calculated with Eqs. (6) and (7), at various temperatures in an Arrhenius plot. Note that several measurements were performed at each temperature. In Fig. 3 we plot the association rate coefficients from flash photolysis of hMbCO and $hMbO_2$. These data together with the measured λ_{app} of the O_2/CO replacement reaction were subsequently used to calculate λ_{-L} for MbO_2 according to Eq. (5). For $hMbO_2$, Fig. 1 shows that ligand escape from the heme pocket after dissociation increases from 48% at 274 K to 92% at 332 K. Therefore, applying Eq. (7) introduces a significant, temperature-dependent correction. The dissociation rate coefficients k_{AB} of $hMbO_2$ are plotted in Fig. 2 together with the hMbCO data.

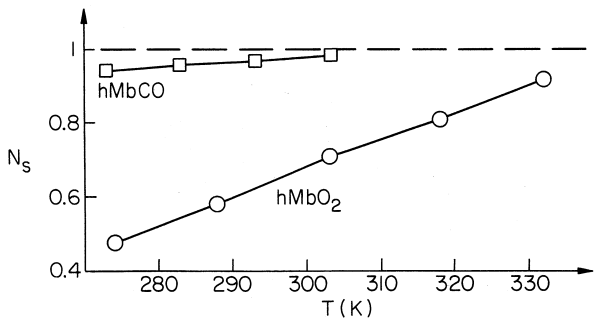

Fig. 1 The fraction of ligands that leaves the heme pocket after photodissociation of hMbCO and $hMbO_2$, N_S, between 274 and 330 K, as determined by transient spectroscopy with nanosecond time resolution

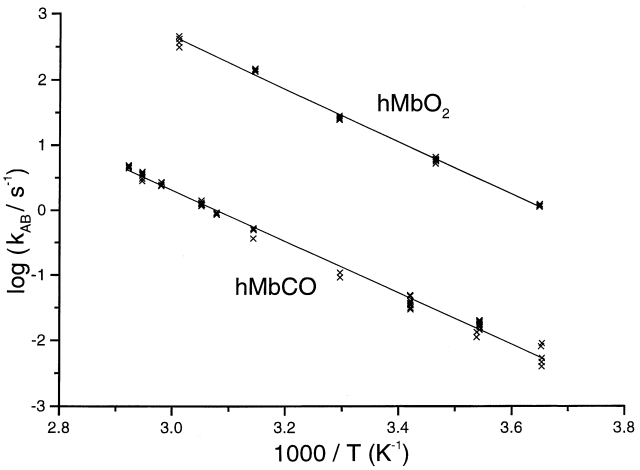

Fig. 2 Arrhenius plots of the dissociation rate coefficients, k_{AB}, of hMbCO and $hMbO_2$, determined by stopped-flow rapid mixing and flash photolysis techniques

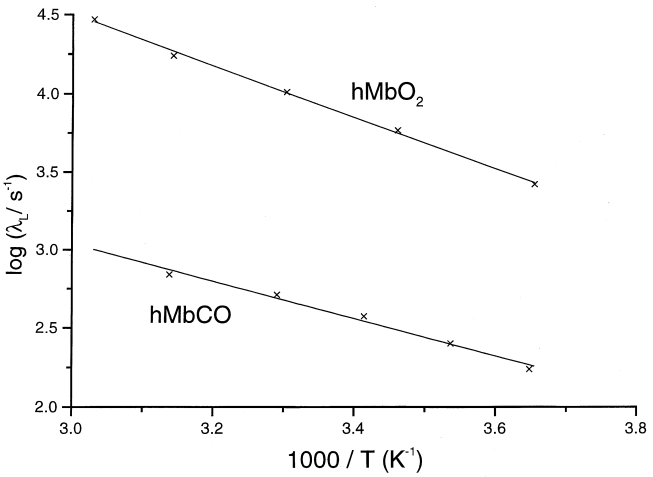

Fig. 3 Arrhenius plot of overall association rate coefficients, λ_L, of hMbCO and $hMbO_2$

4 Data analysis and discussion

Table 1 contains pre-exponentials and activation enthalpies of the dissociation of ligands from hMbCO and $hMbO_2$, and also the association parameters from flash photolysis at low temperatures (Nienhaus et al. 1995). The association data for hMbCO are identical within error to those reported by Doster and coworkers (Post et al. 1993). For comparison, we also include data for sperm whale myoglobin (Beece et al. 1979; Steinbach et al. 1991). The pre-exponentials A_{AB} and activation enthalpies H_{AB} of hMbCO and $hMbO_2$ were obtained with a non-linear least-squares fit of the Arrhenius equation, Eq. (2), to the data in Fig. 2. For both ligands, the fit yields an activation enthalpy of 74 kJ/mol. However, the pre-exponentials of hMbCO and $hMbO_2$ are $10^{11.3}$ s^{-1} and $10^{13.8}$ s^{-1}, respectively. They differ by a factor of 300, and consequently, the higher dissociation rate of $hMbO_2$ arises solely from the larger pre-exponential. Our $hMbO_2$ dissociation parameters are very similar to those from a previous replacement experiment on $swMbO_2$ (Beece et al. 1979). Antonini and Brunori also reported activation enthalpies for the dissociation of CO and O_2 from hMb, citing unpublished work by Antonini, Gibson and Wyman (1965). While their activation enthalpy for hMbCO, 70 kJ/mol, agrees within error with our result, their enthalpy for $hMbO_2$, 80 kJ/mol, is significantly larger. Our data also yield an activation enthalpy of 80 kJ/mol if we omit the correction with Eq. (7). Therefore, we believe that this discrepancy is a direct consequence of the fact that, back in 1965, geminate processes were not yet understood, and the older data were not corrected for incomplete ligand escape. From the activation enthalpies and the dissociation rate coefficients at room temperature that were reported by Antonini and Brunori (1971), we have calculated pre-exponentials with Eq. (2) as $10^{10.2}$ s^{-1} for hMbCO and $10^{14.7}$ s^{-1} for $hMbO_2$. Their data yield an even larger difference in pre-exponentials between the two ligands than our data (as a consequence of the different activation enthalpies) and support our conclusion that the dissociation pre-exponentials for the two ligands are substantially different. By contrast, the association pre-exponentials differ only by a factor of 2.5, and the peak activation enthalpies H_{BA} of the low temperature distributions are identical (Table 1).

What do the different pre-exponentials for the two ligands tell us about the system? The pre-exponential can be written as

$$A = \nu \exp(S/R)\,, \tag{8}$$

where S is the activation entropy, and the frequency factor $\nu = \nu_0 \kappa$. Typically, ν_0 is taken to be $10^{12}-10^{13}$ s^{-1}. The transmission factor κ depends on friction and nonadiabaticity ($0<\kappa<1$). If we assume about equal frequency factors in wells A and B, ν cancels in the ratio of pre-exponentials of the forward and backward reactions,

$$\frac{A_{AB}}{A_{BA}} = \frac{\exp(S_{AB}/R)}{\exp(S_{BA}/R)} = \exp[(S_B - S_A)/R], \tag{9}$$

and we obtain the ratio of the number of states between the dissociated and bound forms, n_B/n_A. Note that this analysis implies that the reaction surface governing the final binding step ($A \rightleftharpoons B$) does not change strongly between cryogenic temperature, where the association parameters were determined, and the region around 300 K, where the dissociation was studied. For hMbCO, the number of states increases by a factor of 125 when the ligand is dissociated. For $hMbO_2$, this number amounts to more than 15,000. Frauenfelder and Wolynes (1985) suggested that the loss of entropy upon binding can be entirely attributed to the loss of translational and rotational entropy of the ligand in the heme pocket plus the spin change of the heme iron. However, this would imply a similar ratio n_B/n_A for CO and O_2. The observed difference in the number of states makes this explanation rather doubtful. Furthermore, the sharpness of infrared lines of photodissociated CO in the heme pocket (Mourant et al. 1993) and two recent x-ray structure analyses (Schlichting et al. 1994; Hartmann et al. 1996) indicate that the ligand resides in a well-defined position in the heme pocket after dissociation, which seems incompatible with estimates of translational entropy loss based on the volume of the heme pocket. The present data point more toward the protein as the source of the entropy difference. The x-ray structure of photodissociated MbCO (Schlichting et al. 1994; Hartmann et al. 1996) shows clear structural differences between the bound and unbound state. Upon binding, the heme iron moves into a well-defined position near the heme plane. The associated structural changes may contribute significantly to the loss of entropy. For MbO_2, we have to consider another effect that leads to an additional loss of entropy. The dioxygen does not only bind to the heme iron but also forms a hydrogen bond to the N_ε atom of the distal histidine (His-E7) (Olson et al. 1988). This additional bond contributes additional binding enthalpy but also restricts librations of the bound ligand and motions of the imidazole sidechain of

Table 1 Arrhenius parameters for the final binding step of CO and O_2 binding to myoglobin

	Dissociation		Association		
System	log (A_{AB}/s^{-1})	H_{AB} (kJ/mol)	log (A_{BA}/s^{-1})	H_{BA}^{peak} (kJ/mol)	log (A_{AB}/A_{BA})
hMbCO	11.3±0.4 [a]	74±2.6 [a]	9.2±0.2 [b]	13 ±0.4 [b]	2.1 [a]
$hMbO_2$	13.8±0.5 [a]	74±3.4 [a]	9.6±0.2 [b]	13 ±0.4 [b]	4.2 [a]
swMbCO	–	–	8.8±0.2 [c]	9.7±0.4 [c]	–
$swMbO_2$	13.6 [d]	73 [d]	8.9±0.3 [c]	9.2±0.6 [c]	–

[a] This work
[b] Data from (Nienhaus et al. 1996)
[c] Data from (Steinbach et al. 1991)
[d] Data from Fig. 5 in (Beece et al. 1979), analyzed with Eq. (2) ($T > 280$ K)

His-E7 inside the heme pocket. Thus an additional loss of entropy upon binding is expected for MbO_2.

While it is straight-forward to calculate the ratio n_B/n_A from the data, the activation entropy $\exp(S/R)$ can only be extracted from A by assuming a frequency factor, ν. For oxygen binding, an adiabatic reaction is expected, with a typical frequency factor of 10^{12} s^{-1}. The data then would imply that, upon binding, about half of the entropy gets lost upon approaching the transition state, and the other half afterwards. In MbO_2, bond formation leads to the polar $Fe^{\delta(+)}-O-O^{\delta(-)}$ complex that hydrogen-bonds to His-E7. Upon approach of the transition state, polarization of the dioxygen may be insufficient for hydrogen bond formation with His-E7. Therefore, the loss of entropy up to the transition state may reflect iron-ligand bond formation only, and the formation of the hydrogen bond will lead to an an additional entropy loss after passing through the transition state.

For CO binding, we cannot assume a frequency factor $\nu = 10^{12}$ s^{-1} *a priori*. From the spin change of two and the weaker second-order spin-orbit coupling between the two diabatic energy surfaces, a much lower frequency factor is expected, indicating that many transitions through the Landau-Zener mixing region occur without spin change. However, the calculation of the electronic matrix element $|V_{qs}|$ that couples the quintet with the singlet state is difficult, and there has been considerable inflation in this parameter over time, starting with Jortner and Ulstrup (1979), who quoted $|V_{qs}| = 1$ cm^{-1}, continuing with Redi et al. (1981) with $|V_{qs}| = 10$ cm^{-1}, and Buhks and Jortner (1985), who calculated $|V_{qs}| = 90$ cm^{-1} and a Landau-Zener parameter $\gamma = 0.3$, implying a reduction of ν by only a factor of three from its adiabatic value. The latter result means that the reaction rate is essentially not affected by the spin change. Indeed, Miers et al. (1991) have observed pre-exponentials as high as $10^{11.5}$ s^{-1} for protoheme-CO. Hence we take $10^{11.5}$ s^{-1} as the frequency factor for hMbCO, and from comparison with the pre-exponential of the dissociation reaction (Table 1) we conclude that a loss of states by a factor of 200 occurs essentially upon approach of the transition state, without any further loss as the product is formed.

In this work, temperature-dependent measurements of the association rate coefficients were necessary for the determination of k_{AB} of $hMbO_2$. In Table 2, we list the parameters that were obtained from a fit of the Arrhenius law, Eq. (2), to the ligand association data in Fig. 3. The fits are given as solid lines in Fig. 3. The association rate coefficient is a complicated, model-dependent function of the microscopic rate coefficients and thus not expected to follow a simple rate theory, such as thermally activated crossing of a single barrier. Nevertheless, Fig. 3 shows that the Arrhenius relation works reasonably well as an empirical parameterization in the fairly narrow temperature range considered (note, however, the curvature in the hMbCO data).

Table 2 Arrhenius parameterization of the overall association of CO and O_2 to horse myoglobin

System	log (A/s^{-1})	H (kJ/mol)
hMbCO	5.7±0.6	20±2
$hMbO_2$	8.5±0.4	29±1

In a sequential model, the association rate coefficient is given by

$$\lambda_L = \langle k_{BA} \rangle \, P_B \, N_S \,, \tag{10}$$

where P_B is the pocket occupation factor, which only weakly depends on temperature, and N_S is close to 1 at higher temperatures (Doster et al. 1982). In this model, the enthalpies in Table 2 should reflect the activation enthalpy of the inner barrier for ligand binding. Note that the enthalpies are much higher than those measured at cryogenic temperature (see Table 1), which can be explained by conformational relaxation ($B^0 \rightarrow B^3$) of the protein after ligand dissociation at higher temperatures (Steinbach et al. 1991; Nienhaus et al. 1992; Ansari et al. 1994). The reaction step $A \rightleftharpoons B^0$ that we have dealt with in this paper is an important intermediate step that governs the dissociation (for $N_S \approx 1$). Bimolecular ligand association, however, occurs from the relaxed state B^3 which has a much higher activation enthalpy than B^0 (Nienhaus et al. 1994).

Acknowledgement We thank Professor H. Frauenfelder and P. G. Wolynes for helpful discussion, and Professor S. Sligar's group for making their stopped-flow spectrometer available to us. This work was supported in part by the National Institutes of Health (Grant GM 18051) and the University of Illinois at Urbana-Champaign.

References

Ahmed AM, Campbell BF, Caruso D, Chance MR, Chavez MD, Courtney SH, Friedman JM, Iben IET, Ondrias MR, Yang M (1991) Evidence for proximal control of ligand specificity in hemeproteins: absorption and raman studies of cryogenically trapped photoproducts of ligand bound myoglobins. Chem Phys 158: 329–352

Alben JO, Beece D, Bowne SF, Doster W, Eisenstein L, Frauenfelder H, Good D, McDonald JD, Marden MC, Moh PP, Reinisch L, Reynolds AH, Shyamsunder E, Yue KT (1982) Infrared spectroscopy of photodissociated carboxymyoglobin at low temperatures. Proc Natl Acad Sci USA 79: 3744–3748

Ansari A, Jones CM, Henry ER, Hofrichter J, Eaton WA (1994) Conformational relaxation and ligand binding in myoglobin. Biochemistry 33: 5128–5145

Antonini E, Brunori M (1971) Hemoglobin and myoglobin in their reactions with ligands. North-Holland, Amsterdam

Austin RH, Beeson KW, Eisenstein L, Frauenfelder H, Gunsalus IC (1975) Dynamics of ligand binding to myoglobin. Biochemistry 14: 5355–5373

Beece D, Eisenstein L, Frauenfelder H, Good D, Marden MC, Reinisch L, Reynolds AH, Sorensen LB, Yue KT (1979) Dioxygen replacement reaction in myoglobin. Biochemistry 15: 3421–3423

Berendzen J, Frauenfelder H, Sauke T, Scholl R (1989) A logarithmic-timebase transient recorder. Bull Am Phys Soc (abst) 34: 880 a

Braunstein DP, Chu K, Egeberg KD, Frauenfelder H, Mourant JR, Nienhaus GU, Ormos P, Sligar SG, Springer BA, Young RD (1993) Ligand binding to heme proteins: III. FTIR studies of His-E7 and Val-E11 mutants of carbonmonoxymyoglobin. Biophys J 65: 2447–2454

Buhks E, Jortner J (1985) The dynamics of carbon monoxide binding to hemoglobin and to cytochrome. J Chem Phys 83: 4456–4462

Campbell BF, Chance MR, Friedman JM (1987) Linkage of functional and structural heterogeneity in proteins: dynamic hole burning in carboxymyoglobin. Science 238: 373–376

Champion PM (1988) Cytochrome P450 and the transform analysis of heme protein Raman spectra. In: Spiro TG (ed) Biological applications of Raman spectroscopy. Wiley, New York, pp 249–292

Chance MR, Courtney SH, Chavez MD, Ondrias MR, Friedman JM (1990) O_2 and CO reactions with heme proteins: quantum yields and geminate recombination on piosecond time scales. Biochemistry 29: 5537–5545

Chatfield MD, Walda KN, Magde D (1990) Activation parameters for ligand escape from myoglobin proteins at room temperature. J Am Chem Soc 112: 4680–4687

Doster W, Beece D, Bowne SF, DiIorio EE, Eisenstein L, Frauenfelder H, Reinisch L, Shyamsunder E, Winterhalter KH, Yue KT (1982) Control and pH dependence of ligand binding to heme proteins. Biochemistry 21: 4831–4839

Frauenfelder H, Wolynes PG (1985) Rate theories and puzzles of heme protein kinetics. Science 229: 337–345

Gibson QH (1959) The kinetics of reactions between haemoglobin and gases. In: Progr Biophys Biophys Chem vol 9. Pergamon Press, New York, pp 1–53

Gilch H, Schweitzer-Stenner R, Dreybrodt W (1993) Structural heterogeneity of the Fe^{2+}-$N_{\varepsilon}(His^{F8})$ bond in various hemoglobin and myoglobin derivatives probed by the Raman-active iron histidine stretching mode. Biophys J 65: 1470–1485

Hartmann H, Zinser S, Komninos P, Schneider RT, Nienhaus GU, Parak F (1996) X-ray structure determination of a metastable state of carbonmonoxy myoglobin after photodissociation. Proc Natl Acad Sci USA 93: 7013–7016

Jortner J, Ulstrup J (1979) Dynamics of nonadiabatic atom transfer in biological systems. Carbon monoxide binding to hemoglobin. J Am Chem Soc 101: 3744–3754

Kuriyan J, Wilz S, Karplus M, Petsko GA (1986) X-ray structure and refinement of carbon-monoxy (Fe II)-myoglobin at 1.5 Å resolution. J Mol Biol 192: 133–154

Li T, Quillin ML, Phillips Jr GN, Olson JS (1994) Structural determinants of the stretching frequency of CO bound to myoglobin. Biochemistry 33: 1433–1446

Lim M, Jackson TA, Anfinrud PA (1993) Nonexponential protein relaxation: dynamics of conformational change in myoglobin. Proc Natl Acad Sci USA 90: 5801–5804

Miers JB, Postlewaite JC, Cowen BR, Roemig GR, Lee IS, Dlott DD (1991) Preexponential-limited solid state chemistry: ultrafast rebinding of a heme-ligand complex in a glass or protein matrix. J Chem Phys 94: 1825–1836

Mourant JR, Braunstein DP, Chu K, Frauenfelder H, Nienhaus GU, Ormos P, Young RD (1993) Ligand binding to heme proteins: II. Transitions in the heme pocket of myoglobin. Biophys J 65: 1496–1507

Nienhaus GU, Chu K, McMahon B, Müller JD (1995) Conformational relaxation and ligand binding in heme proteins. In: Sarma RH, Sarma MH (eds) Biological Structure and Dynamics, vol 1. Adenine Press, Albany, NY, pp 281–296

Nienhaus GU, Mourant JR, Chu K, Frauenfelder H (1994) Ligand binding to heme proteins. The effect of light on ligand binding in myoglobin. Biochemistry 33: 13 413–13 430

Nienhaus GU, Mourant JR, Frauenfelder H (1992) Spectroscopic evidence for conformational relaxation in myoglobin. Proc Natl Acad Sci USA 89: 2902–2906

Olson JS (1981) Stopped-flow, rapid mixing measurements of ligand binding to hemoglobin and red cells. In: Methods enzym, vol 76. Academic Press, New York, NY, pp 631–651

Olson JS, Mathews AJ, Rohlfs RJ, Springer BA, Egeberg KD, Sligar SG, Tame J, Renaud J-P, Nagai K (1988) The role of the distal histidine in myoglobin and haemoglobin. Nature 336: 265–266

Petrich JW, Poyart C, Martin JL (1988) Photophysics and reactivity of heme proteins: A femtosecond absorption study of hemoglobin, myoglobin, and protoheme. Biochemistry 27: 4049–4060

Phillips SEV (1980) Structure and refinement of oxymyoglobin at 1.6 Å resolution. J Mol Biol 142: 531–554

Post F, Doster W, Karvounis G, Settles M (1993) Structural relaxation and nonexponential kinetics of CO-binding to horse myoglobin – multiple flash photolysis experiments. Biophys J 64: 1833–1842

Redi M, Gerstman BS, Hopfield JJ (1981) Hemoglobin-carbob monoxide binding rate. Low temperature magneto-optical detection of spin-tunneling. Biophys J 35: 471–484

Rousseau DL, Argade PV (1986) Metastable photoproducts from carbon monoxide myoglobin. Proc Natl Acad Sci USA 83: 1310–1314

Schlichting I, Berendzen J, Phillips Jr GN, Sweet RM (1994) Crystal structure of photolysed carbonmonoxy-myoglobin. Nature 371: 808–812

Shimada H, Caughey WS (1982) Dynamic protein structures: Effects of pH on conformer stabilities at the ligand-binding site of bovine heartmyoglobin carbonyl. J Biol Chem 257: 11 893–11 900

Steinbach PJ, Ansari A, Berendzen J, Braunstein D, Chu K, Cowen BR, Ehrenstein D, Frauenfelder H, Johnson JB, Lamb DC, Luck S, Mourant JR, Nienhaus GU, Ormos P, Philipp R, Xie A, Young RD (1991) Ligand binding to heme proteins: the connection between dynamics and function. Biochemistry 30: 3988–4001

Teng T-Y, Srajer V, Moffat K (1994) Photolysis-induced structural changes in single crystals of carbonmonoxy myoglobin at 40 K. Nature Struct Biol 1: 701–705

Yang F, Phillips Jr GN (1996) Crystal structures of CO-, deoxy- and met-myoglobins at various pH values. J Mol Biol 256: 762–774